

## Rational Design of a Covalently Tethered Dinuclear $[\text{Mn}^{\text{II}}(\text{N}_3\text{O}_2)\text{Cl}(\text{OH}_2)]_2^{2+}$ Macrocyclic Building Block: Synthesis, Structure, and Magnetic Properties

Jian Wang,<sup>†</sup> Brianna Slater,<sup>†</sup> Antonio Alberola,<sup>‡</sup> Helen Stoeckli-Evans,<sup>§</sup> Fereidoon S. Razavi,<sup>†</sup> and Melanie Pilkington<sup>\*†</sup>

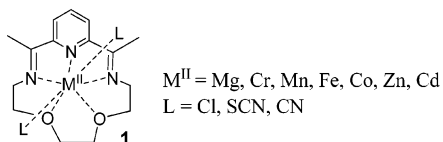
Department of Chemistry, Brock University, 500 Glenridge Avenue, St. Catharines, L2S 3A1 Ontario, Canada, Departamento de Química Física y Analítica, Universitat Jaume I, Avenida Sos Baynat s/n, 12701 Castellón, Spain, and Institut de Microtechnique, Rue Emile-Argand 11, Bâtiment G, Case Postal 158, CH-2009 Neuchâtel, Switzerland

Received November 20, 2006

A novel dimeric  $\text{Mn}^{\text{II}}$  complex  $\{[\text{Mn}(\text{N}_3\text{O}_2)\text{Cl}(\text{OH}_2)]_2\text{Cl}\}$  (**2**) of a macrocyclic Schiff base ligand derived from the condensation of 2,2',6,6'-tetraacetyl-4,4'-bipyridine with 3,6-dioxaoctane-1,8-diamine in the presence of a stoichiometric amount of  $\text{Mn}^{\text{II}}$  has been prepared and characterized. The X-ray analysis of **2** reveals that the two Mn ions assume a pentagonal-bipyramidal geometry, with the macrocycle occupying the pentagonal plane and the axial positions being filled by a halide ion and a  $\text{H}_2\text{O}$  molecule. Magnetic susceptibility data (2–270 K) reveal the occurrence of weak antiferromagnetic interactions between covalently tethered  $\text{Mn}^{\text{II}}\text{--Mn}^{\text{II}}$  dimeric units.

In recent years, developing new synthetic strategies for the preparation of molecule-based magnetic materials has become an important area of research.<sup>1</sup> One synthetic rationale commonly employed is the use of organic molecules, e.g., macrocycles, to block several of the coordination sites of the assembling paramagnetic cations. Macrocyclic ligands are usually coordinated into the equatorial plane of the metal ions, leaving two free axial positions that can be occupied by bridging ligands, which, in turn, can function as organic linkers between adjacent paramagnetic metal centers.<sup>2,3</sup>

In 1977, Nelson reported metal complexes of a 15-membered Schiff base macrocyclic ligand **1**.<sup>4a</sup> Interest in this



macrocyclic ligand has gained momentum in recent years

\* To whom correspondence should be addressed. E-mail: mpilkington@brocku.ca.

<sup>†</sup> Brock University.

<sup>‡</sup> Universitat Jaume I.

<sup>§</sup> Institut de Microtechnique.

given that the  $\text{Fe}^{\text{II}}$  complex  $[\text{Fe}^{\text{II}}(\text{L})(\text{CN})_2]\cdot\text{H}_2\text{O}$  exhibits spin-crossover behavior ( $S = 0 \leftrightarrow S = 2$ ) including a LIESST effect, with a high relaxation temperature of 130 K.<sup>5</sup> A number of divalent cations have been successfully employed as metal templates for the formation of the  $\text{N}_3\text{O}_2$  macrocycle **1**,<sup>3,4</sup> but no successful transmetalation reactions have been reported to date for complexes of this particular macrocycle. Nevertheless, mononuclear complexes have recently become popular as connection devices for self-assembly, a strategy that has been successfully exploited for the preparation of magnetic clusters as well as 1- and 2-D coordination polymers.<sup>3</sup> Given these advances, a new class of compound incorporating Nelson's  $\text{N}_3\text{O}_2$  macrocycle **1** should serve as a useful building block for exploitation in the field of supramolecular chemistry.

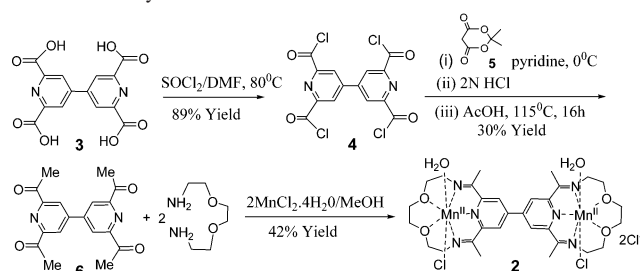
We report herein the synthesis, structure, and magnetic properties of a new bimetallic Schiff base compound comprised of two covalently tethered  $\text{N}_3\text{O}_2$  pentadentate macrocycles built around a 4,4'-bipyridine moiety  $\{[\text{Mn}(\text{N}_3\text{O}_2)\text{Cl}\cdot\text{H}_2\text{O}]_2\text{Cl}\cdot 10.5\text{H}_2\text{O}\}$  (**2**). Synthetic routes to covalently tethered macrocycles are relatively uncommon in the chemical literature. Nevertheless, their potential as ligand systems for

- (1) (a) *Magnetic Molecular Materials*; Gatteschi, D., Khan, O., Miller, J. S., Palacio, F., Eds.; NATO ASI Series G198; Kluwer Academic Publishers: Dordrecht, The Netherlands, 1989. (b) Mrozinski, J. *Coord. Chem. Rev.* **2005**, *249*, 2534.
- (2) Lindsay, L. F. *The Chemistry of Macrocyclic Ligand Complexes*; Cambridge University Press: Cambridge, U.K., 1989.
- (3) (a) Hayami, S.; Jahanz, G.; Maeda, Y.; Yokoyama, T.; Osamu, S. *Inorg. Chem.* **2005**, *44*, 7289–7291. (b) Parashiv, C.; Andrich, M.; Journaux, Y.; Zak, Z.; Kyritasakag, M.; Ricard, L. *J. Mater. Chem.* **2006**, *16*, 2660–2668. (c) Bonadio, F.; Senna, M.-C.; Ensling, J.; Sieber, A.; Neels, A.; Stoeckli-Evans, H.; Decurtins, S. *Inorg. Chem.* **2005**, *44*, 969–978.
- (4) Drew, M. G. B.; Othman, A. H. B.; McFau, S. G.; Meilrey, P. D. A.; Nelson, M. D. *J. Chem. Soc., Dalton Trans.* **1977**, 1173–1180. Nelson, S. M.; McIlray, P. D. A.; Stevenson, C. S.; König, E.; Ritter, G.; Waigel, J. *J. Chem. Soc., Dalton Trans.* **1986**, 991.
- (5) Hayami, S.; Gu, Z.-Z.; Einaga, Y.; Kobayashi, Y.; Ishikawa, Y.; Yamada, Y.; Fujishima, A.; Sato, O. *Inorg. Chem.* **2001**, *40*, 3240–3242.

**Table 1.** Crystallographic Data for Compound **2**

empirical formula	C <sub>30</sub> H <sub>65</sub> Cl <sub>4</sub> Mn <sub>2</sub> N <sub>6</sub> O <sub>16.5</sub>
fw	1025.56
<i>T</i> , K	173(2)
$\lambda$ , Å	0.710 73
space group	<i>P</i> $\bar{1}$
<i>a</i> , Å	11.1004(9)
<i>b</i> , Å	14.6062(12)
<i>c</i> , Å	17.2490(13)
$\alpha$ , deg	63.667(6)
$\beta$ , deg	70.728(6)
$\gamma$ , deg	77.087(6)
<i>V</i> , Å <sup>3</sup>	2356.2(3)
<i>Z</i>	2
$\rho_{\text{calc}}$ , g cm <sup>-3</sup>	1.447
$\mu$ , mm <sup>-1</sup>	0.831
<i>R</i> ( <i>F</i> <sup>2</sup> ) <sup>a</sup>	0.0799
<i>R</i> <sub>w</sub> ( <i>F</i> <sup>2</sup> ) <sup>b</sup>	0.1988

$$^a R = \frac{\sum ||F_o| - |F_c||}{\sum |F_o|}. \quad ^b R_w = \frac{[\sum w(|F_o|^2 - |F_c|^2)^2]}{\sum w|F_o|^4}]^{1/2}.$$

**Scheme 1.** Synthetic Route to **2**

preparing compounds with intermolecular magnetic interactions when bridging ligands are installed provides an attractive approach for the preparation of extended systems that could yield novel materials such as molecule-based magnets.

The preparation and crystal growth of **2** is as follows. 2,2',6,6'-Tetraacetyl-4,4'-bipyridine (**6**; 0.162 g, 0.50 mmol) was added to a solution of MnCl<sub>2</sub>·4H<sub>2</sub>O (0.148 g, 1.00 mmol) in methanol (MeOH; 10 mL). The mixture was kept at 50 °C, and a solution of 3,6-dioxaoctane-1,8-diamine (0.198 g, 1.00 mmol) in MeOH (5 mL) was added with continuous stirring. The resulting solution was then refluxed for 6 h, after which time the solvent was partially removed and the resulting solid was isolated by filtration, washed with diethyl ether, and air-dried to afford the product as an orange/brown solid. Yield: 42%. IR (KBr, cm<sup>-1</sup>): 3423 br (OH), 2928–2883 s, 1646 s (C=N), 1105–1073 s (C–O–C), 1597 s, 877 m, 660 w (py). MS (FAB): *m/z* 763 [M – H]<sup>+</sup>, 728 [M – 2H<sub>2</sub>O]<sup>+</sup> (100%). Anal. Calcd for C<sub>30</sub>H<sub>65</sub>N<sub>6</sub>O<sub>16.5</sub>Cl<sub>4</sub>Mn<sub>2</sub>: C, 35.1; H, 6.4; N, 8.2. Found: C, 35.4; H, 6.4; N, 8.1. Small orange plates suitable for X-ray crystallography were grown via slow evaporation of a MeOH solution at room temperature.

Intensity data were collected at 173 K on a Stoe Mark II image plate diffraction system using graphite-monochromated Mo K $\alpha$  radiation.<sup>6</sup> A semiempirical absorption correction using the program *PLATON/MULABS*<sup>7</sup> was applied to the data for **2**. The structure was solved by direct methods using the program *SHELXS-97*.<sup>8</sup> The refinement and all

**Figure 1.** ORTEP<sup>12</sup> representation of the molecular structure of **2** (ellipsoids at 50% probability). The Cl<sup>-</sup> counterions are omitted for clarity.**Table 2.** Selected Bond Distances (Å) and Bond Angles (deg) for **2**

Mn1–N1	2.119(5)	Mn2–N4	2.124(5)
Mn1–N2	2.182(5)	Mn2–N5	2.194(5)
Mn1–N3	2.184(5)	Mn2–N6	2.180(5)
Mn1–O1	2.242(4)	Mn2–O3	2.273(4)
Mn1–O2	2.272(4)	Mn2–O4	2.273(4)
Mn1–O1W	2.127(5)	Mn2–O2W	2.108(5)
Mn1–Cl1	2.474(2)	Mn2–Cl2	2.465(2)
N1–Mn1–N3	72.52(18)	N4–Mn2–N6	72.95(17)
N3–Mn1–O2	72.14(17)	N6–Mn2–O4	71.77(15)
O2–Mn1–O1	71.07(15)	O4–Mn2–O3	70.95(14)
O1W–Mn1–Cl1	178.99(17)	O2W–Mn2–Cl2	174.05(15)

further calculations were carried out using *SHELXL-97*.<sup>9</sup> *PLATON/SQUEEZE*<sup>7</sup> was used to correct the data for the presence of the disordered solvent. Crystallographic data for compound **2** are summarized in Table 1.

The synthetic route for the preparation of the macrocycle is outlined in Scheme 1. The known tetraacid **3**<sup>10</sup> was converted to tetrachloroformyl-4,4'-bipyridine (**4**) by reaction with thionyl chloride in *N,N*-dimethylformamide.<sup>11</sup> The reaction of **4** with 2,2-dimethyl-1,3-dioxane-4,6-dione (**5**, Meldrum's acid) followed by hydrolysis and decarboxylation afforded **6**.<sup>11</sup> Compound **6** then undergoes a metal-templated Schiff base condensation reaction together with 3,6-dioxaoctane-1,8-diamine to give the desired covalently tethered macrocycle **2**.<sup>4</sup> A  $\nu(\text{C}=\text{N})$  stretching mode was observed at 1646 cm<sup>-1</sup> in the IR spectrum of **2** that supports imine formation. A peak in the fast atom bombardment (FAB) mass spectrum at *m/z* 763 is also consistent with the loss of a proton from the [Mn(N<sub>3</sub>O<sub>2</sub>)Cl(H<sub>2</sub>O)]<sub>2</sub><sup>2+</sup> species.

The molecular structure of **2** was determined by X-ray crystallography and consists of two tethered N<sub>3</sub>O<sub>2</sub> pentadentate macrocycles chelated to Mn<sup>II</sup> metal ions, together with four Cl<sup>-</sup> anions (two coordinated and two uncoordinated, one of which is disordered over two sites) and two coordinated water molecules. The molecular structure together with the atomic numbering scheme is shown in Figure 1. Selected bond distances and angles are given in Table 2.

Both Mn<sup>II</sup> ions are in a pentagonal-bipyramidal environment, with the macrocycles occupying the equatorial plane

(8) Sheldrick, G. M. *SHELXS-96*, Program for Crystal Structure Determination. *Acta Crystallogr.* **1990**, *A46–A47*, 473.

(9) Sheldrick, G. M. *SHELXL-97*; Universitat Göttingen: Göttingen, Germany, 1999.

(10) Pryer, K. E.; Shipps, G. W.; Skyler, D. A.; Rebek, J. *Tetrahedron*. (11) Fallahpour, R. A.; Neuburger, M.; Zehnder, M. *Polyhedron* **1999**, *18*, 2445–2454.

(6) Stoe. X-Area version 1.26 and X-RED32 version 1.26 software; Stoe and Cie GmbH: Darmstadt, Germany, 2005.

(7) Spek, A. L. *J. Appl. Crystallogr.* **2003**, *36*, 7–13.

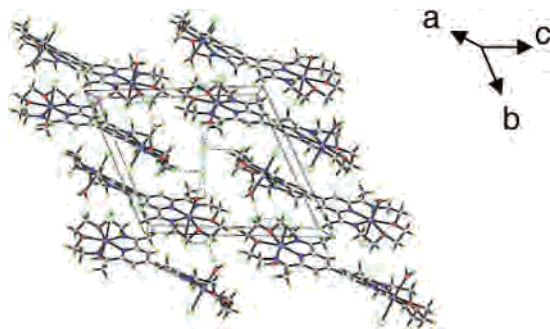


Figure 2. Packing diagram for **2** viewed down the *a* axis.

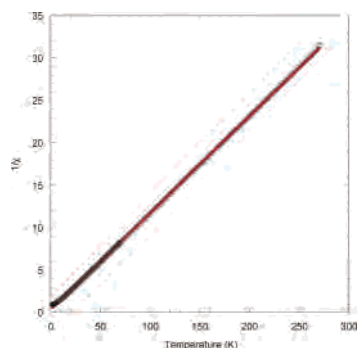


Figure 3.  $1/\chi$  including a fit to the Curie–Weiss law.

and a bound water molecule and  $\text{Cl}^-$  ion in the axial positions. The dihedral angle between the two planes of the pyridine rings is  $41^\circ$ . The two macrocyclic rings are nearly planar. The maximum deviations of contributing atoms from the  $\text{Mn}(\text{N}_3\text{O}_2)$  least-squares plane are  $0.1 \text{ \AA}$  (N3) and  $0.1 \text{ \AA}$  (N6). The distance between the two  $\text{Mn}^{\text{II}}$  ions in the molecule is  $11.2 \text{ \AA}$ . The packing diagram reveals that centrosymmetric pairs of molecules are stacked along the *c* axis (Figure 2). The shortest distance between neighboring pyridine rings is  $5.46 \text{ \AA}$ . Intermolecular contacts between  $\text{Cl}^-$  anions and neighboring H atoms are in the range of  $2.87\text{--}3.11 \text{ \AA}$  and are shown as dashed lines. Compound **2** was magnetically characterized by following the temperature dependence of the magnetic susceptibility.<sup>13</sup> The susceptibility of the sample rises monotonically as the temperature is decreased following a typical Curie–Weiss behavior, from which the Curie constant *C* could be determined. The presence of two  $\text{Mn}^{\text{II}}$  ions per molecule is confirmed by a Curie constant of  $8.741 \text{ emu}\cdot\text{K}/\text{Oe}\cdot\text{mol}$  (as expected for two  $S = 5/2$  and  $g = 2$ ) and a value for the Weiss constant of  $\theta = -2.89 \text{ K}$  (Figure 3). As shown in Figure 4, the  $\chi T$  product is fairly constant between 270 and 45 K at  $8.58 \text{ emu}\cdot\text{K}/\text{Oe}\cdot\text{mol}$  and decreases below 40 K to reach a value of  $1.9 \text{ emu}\cdot\text{K}/\text{Oe}\cdot\text{mol}$  at 2 K. This decrease can arise from either inter- or intradimer coupling. In our view, the dimers are magnetically well isolated, and at the simplest level, we can apply the results

(12) ORTEP-3 for Windows: Farruga, L. J. *J. Appl. Crystallogr.* **1997**, *30*, 565.

(13) Variable-temperature magnetic susceptibility data were collected on a powdered sample of **2** with the use of a Quantum Design SQUID magnetometer in an applied field of 5000 G between 2 and 270 K. Data were corrected for both sample diamagnetism (Pascal's constants) and the sample holder.

(14) Carlin, R. L. *Magnetochemistry*; Springer-Verlag: Heidelberg, Germany, 1986.

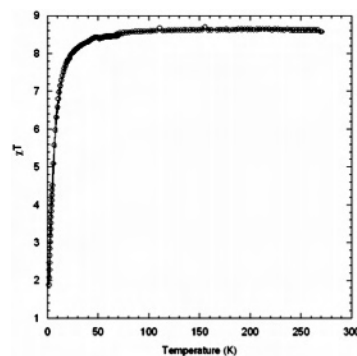


Figure 4.  $\chi T$  vs *T* plot and fit with parameters in the text.

of Weiss's mean-field theory<sup>13</sup> to the measured Weiss constant in order to estimate  $J_{\text{ex}}$  according to eq 1. In eq 1,

$$\theta = [2zJ_{\text{ex}}S(S + 1)]/3k_{\text{B}} \quad (1)$$

*z* is the number of nearest neighbors ( $z = 1$  for a dimer),  $J_{\text{ex}}$  is the exchange interaction between neighbors, and *S* is the spin quantum number. For compound **1**,  $S = 5/2$  and  $\theta = -2.89 \text{ K}$ , from which  $J_{\text{ex}}/k_{\text{B}} \approx -0.49 \text{ K}$ . The magnetic susceptibility can be fit using eq 2 on the basis of the appropriate isotropic Heisenberg Hamiltonian:

$$\hat{H} = -J\hat{S}_{\text{Mn1}}\hat{S}_{\text{Mn2}} \quad \left(S_{\text{Mn1}} = S_{\text{Mn2}} = \frac{5}{2}\right)$$

$$\chi_{\text{m}} = \frac{NG^2\beta^2}{3kT} \frac{55 + 30e^{-5J/kT} + 14e^{-9J/kT} + 5e^{-12J/kT} + e^{-14J/kT}}{11 + 9e^{-5J/kT} + 7e^{-9J/kT} + 5e^{-12J/kT} + 3e^{-14J/kT} + e^{-15J/kT}} \quad (2)$$

A single parameter curve fit to the expression for  $\chi$  in compound **2** yielded  $J_{\text{ex}} = -0.51 \text{ K}$  with  $g = 2$ , which is in very good agreement with the estimate from the mean-field theory (Figure 4) and is suggestive that the intradimer coupling is dominant. However, the weak nature of these interactions makes it impossible to completely rule out that interdimer interactions could also play a role in the magnetic properties.

To summarize, we have developed a new synthetic strategy to a magnetic building block comprising two covalently tethered pentadentate  $\text{Mn}^{\text{II}}$  macrocycles. Structural characterization reveals that the  $\text{Mn}^{\text{II}}$  ions contain labile axial ligands that can be readily replaced by bridging ligands, e.g., cyanide. Work along these lines is currently in progress and will be reported in due course.

**Acknowledgment.** This work was supported by the NSERC, CRC, Brock University (BUSRA, International Seed Funds), and the MEC (Ramon y Cajal research contract to A.A.).

**Supporting Information Available:** X-ray crystallographic files in CIF format for compound **1**. This material is available free of charge via the Internet at <http://pubs.acs.org>.

IC0622120